



CM-P00064261

PRINT 77-0871-CERN

STUDY OF INCLUSIVE NEUTRAL CURRENT INTERACTIONS OF NEUTRINOS AND ANTINEUTRINOS

M. Holder, J. Knobloch, J. May, H.P. Paar, P. Palazzi, F. Ranjard,
D. Schlatter, J. Steinberger, H. Suter, H. Wahl, S. Whitaker
and E.G.H. Williams
CERN, Geneva, Switzerland

F. Eisele, C. Geweniger, K. Kleinknecht, G. Spahn and H-J. Willutzki
Institut für Physik*) der Universität, Dortmund, Germany

W. Dorth, F. Dydak, V. Hepp, K. Tittel and J. Wotschack
Institut für Hochenergiephysik*) der Universität, Heidelberg, Germany

P. Bloch, B. Devaux, M. Grimm, J. Maillard,
B. Peyaud, J. Rander, A. Savoy-Navarro and R. Turley
D.Ph.P.E., CEN-Saclay, France

F.L. Navarra
Istituto di Fisica dell'Università, Bologna, Italy

ABSTRACT

We report on results from a study of hadron-energy distributions for ν and $\bar{\nu}$ inclusive neutral current interactions. There is no significant variation of the neutral to charged current total cross-section ratios R_ν and $R_{\bar{\nu}}$ with neutrino energy. The space-time structure of neutral currents is dominated by V-A, with a significant admixture of V+A. The Weinberg-Salam model is in agreement with all data if $\sin^2\theta_w = 0.24 \pm 0.02$.

Geneva - 25 September 1977

*) Supported by Bundesministerium für Forschung und Technologie

1. INTRODUCTION

In a previous letter¹⁾ we have reported on the ratio of the neutral current (NC) to charged current (CC) inclusive cross-section, both for neutrinos (R_ν) and antineutrinos ($R_{\bar{\nu}}$), with a 12 GeV cut-off in hadron-energy. Here we report additional results from a study of the hadron-energy distribution of the same sample of events. The data have been analysed to answer the following questions:

1. What are the values of R_ν and $R_{\bar{\nu}}$ without cut-off in hadron-energy?
2. What is the dependence of R_ν and $R_{\bar{\nu}}$ on neutrino energy?
3. What is the NC y -distribution?
4. Is the neutrino in the initial and final state the same?
5. Is there a significant S or P coupling in the NC interaction?
6. What is the V, A structure of the NC interaction?
7. Is the NC structure compatible with the Weinberg-Salam model?

The data have been obtained in ν and $\bar{\nu}$ narrow-band beams with an incident energy spectrum in the range 12 - 200 GeV. For details about the beam and the detector we refer to reference 2. For each event the hadron-energy E_H is measured as well as its radial distance R to the beam centre. The ν and $\bar{\nu}$ events have been binned into a (10 x 4) matrix, with ten bins of 20 GeV in E_H , and four bins of 40 cm in R . The analysis makes use of the fact that for each radial bin the incident energy spectrum is known, as shown in Fig. 1.

The procedure to obtain the corrected NC and CC event sample has been described previously¹⁾, but now the method is applied to each bin of the (E_H, R) matrix. However, the wide-band beam (WBB) background subtraction has been treated differently because of the limited statistics of events recorded in "closed collimator" runs: preserving the total number of background events observed, scaled up by the flux ratio, they have been re-distributed smoothly over the matrix bins with a E_H distribution parametrized like $\exp(-E_H/10 \text{ GeV})$, and with the number of events per radial bin proportional to its area. These assumptions are in line with the characteristics of the observed "closed collimator" events, and with a Monte Carlo simulation of the WBB background.

The resulting distributions of corrected NC and CC event numbers are

shown in Fig. 2. Instead of working directly with the NC event numbers we have chosen to work with the ratios of NC to CC event numbers. This has the advantage that most of the experimental uncertainties cancel since NC and CC events share the same neutrino spectrum, and much of the data reduction procedure. The obtained ratios of NC to CC event numbers are shown in Fig. 3. We conclude that the NC and CC y -distributions do not differ greatly, and that the ratio of the NC to CC cross-section is not substantially dependent on neutrino energy.

In subsequent sections, in order to gain insight into the NC structure, the data must necessarily be compared with definite functional forms of the y -dependence. For these we have chosen the forms suggested by the quark-parton model. However, the validity of the conclusions in general go beyond the confines of this model. The analysis is performed by comparing Monte Carlo calculations with the data. They translate the predictions of any functional form into (E_H, R) matrices, taking into account the detector geometry, the cuts applied, the experimental resolution, and the kinematics of the neutrino beam.

2. MEASUREMENT OF THE ENERGY-DEPENDENCE AND THE y -DISTRIBUTION OF THE NEUTRAL CURRENT CROSS-SECTION

In this section we deal only with results which are obtained from separate fits of ν and $\bar{\nu}$ data. For these fits we have chosen the following parametrization:

$$\left. \begin{aligned} \frac{NC}{CC}(y) &= R_o \frac{1 + \alpha_{NC}(1-y)^2}{1 + \alpha_{CC}(1-y)^2} && \text{for } \nu \\ &= \bar{R}_o \frac{(1-y)^2 + \bar{\alpha}_{NC}}{(1-y)^2 + \bar{\alpha}_{CC}} && \text{for } \bar{\nu} \end{aligned} \right\} \quad (1)$$

α_{CC} and $\bar{\alpha}_{CC}$ denote in the quark-parton model the antiquark-quark ratio. However, we prefer α_{CC} and $\bar{\alpha}_{CC}$ to be considered as empirically determined input parameters. Since their value is experimentally known to be of the order 0.1 and independent of energy³⁾, we have used in all fits of this section $\alpha_{CC} = \bar{\alpha}_{CC} = 0.10$, but quote also results for

$\alpha_{CC} = \bar{\alpha}_{CC} = 0.15$ when appropriate. The variable fit parameters are R_0 (\bar{R}_0) and α_{NC} ($\bar{\alpha}_{NC}$), which describe the strength of the NC interaction and the shape of its y -distribution, respectively.

2.1 R_ν and $R_{\bar{\nu}}$ without cut-off in hadron-energy

The direct experimental result¹⁾ gives the NC to CC ratios only subject to the cut $E_H > 12$ GeV:

$$\left. \begin{aligned} R_\nu &= 0.293 \pm 0.010 \quad (0.006) \\ R_{\bar{\nu}} &= 0.35 \pm 0.03 \quad (0.021) \end{aligned} \right\} E_H > 12 \text{ GeV}$$

From Eq. 1 we find for the total cross-section ratios of NC to CC without cut-off in hadron-energy:

$$\left. \begin{aligned} R_\nu &= R_0 \frac{3 + \alpha_{NC}}{3 + \alpha_{CC}} = 0.295 \pm 0.010(0.006) \\ R_{\bar{\nu}} &= \bar{R}_0 \frac{1 + 3\bar{\alpha}_{NC}}{1 + 3\bar{\alpha}_{CC}} = 0.34 \pm 0.03(0.017) \end{aligned} \right\} E_H > 0 \text{ GeV}$$

Throughout this paper, the quoted error includes the estimate of the systematic uncertainty. For comparison, the statistical error is given in brackets.

2.2 Dependence of R_ν and $R_{\bar{\nu}}$ on neutrino energy

In order to study the possible energy dependence of R_ν and $R_{\bar{\nu}}$ the data are fit with two parameters R_0 (\bar{R}_0) in Eq. 1, one for $E_\nu < 100$ GeV and the other for $E_\nu > 100$ GeV, but with α_{NC} ($\bar{\alpha}_{NC}$) independent of energy. The results are summarised in Table 1. The ratios $R_\nu(E_\nu > 100 \text{ GeV})/R_\nu(E_\nu < 100 \text{ GeV}) = 0.99 \pm 0.07$ for ν , and $R_{\bar{\nu}}(E_{\bar{\nu}} > 100 \text{ GeV})/R_{\bar{\nu}}(E_{\bar{\nu}} < 100 \text{ GeV}) = 1.03 \pm 0.18$ for $\bar{\nu}$ do not favour a substantial energy dependence. The average observed neutrino energy is 60 GeV below 100 GeV, and 150 GeV above.

2.3 The shape of the NC y -distribution

In Eq. 1 the shape of the NC y -distribution is characterized by α_{NC} ($\bar{\alpha}_{NC}$), to be compared to the corresponding value of α_{CC} ($\bar{\alpha}_{CC}$). The fit results for α_{NC} ($\bar{\alpha}_{NC}$) are dependent on the chosen α_{CC} ($\bar{\alpha}_{CC}$), and are given in Table 2 for $\alpha_{CC} = \bar{\alpha}_{CC} = 0.10$ and $\alpha_{CC} = \bar{\alpha}_{CC} = 0.15$, respectively. The resulting NC shape parameters are i) small compared.

to unity, ii) the same for ν and $\bar{\nu}$ within the experimental error, and iii) not very different from the CC shape parameters α_{CC} and $\bar{\alpha}_{CC}$. The NC and CC shape parameters are in fact consistent within the experimental error. This indicates that the NC structure is dominated by V-A. However, the best fit favours a NC y -distribution which is steeper than the CC y -distribution for ν , and flatter for $\bar{\nu}$.

2.4 Neutrino identity

In NC reactions, the outgoing neutrino is unobserved, and it is reasonable to ask if the incoming and outgoing neutrinos are identical. It has been pointed out by Wolfenstein⁴⁾ that the differential cross-sections $\frac{d\sigma_\nu}{dy}$ and $\frac{d\sigma_{\bar{\nu}}}{dy}$ must coincide at $y = 0$ if the two neutrinos are the same. It has been shown that for CC charge symmetry holds within the experimental error, i.e., $\frac{d\sigma_\nu}{dy} = \frac{d\sigma_{\bar{\nu}}}{dy}$ at $y = 0$ ³⁾. So one expects in case of ν identity from Eq. 1:

$$R_o \frac{1 + \alpha_{NC}}{1 + \alpha_{CC}} = \bar{R}_o \frac{1 + \bar{\alpha}_{NC}}{1 + \bar{\alpha}_{CC}} .$$

We find

$$R_o \frac{1 + \alpha_{NC}}{1 + \alpha_{CC}} = 0.313 \pm 0.033(0.026)$$

$$\bar{R}_o \frac{1 + \bar{\alpha}_{NC}}{1 + \bar{\alpha}_{CC}} = 0.297 \pm 0.034(0.028)$$

which gives

$$\left[\frac{d\sigma_{\bar{\nu}}}{dy} / \frac{d\sigma_\nu}{dy} \right]_{y=0}^{\text{Fe target}} = 0.95 \pm 0.15(0.12)$$

assuming strict charge symmetry for CC. This result supports the concept of neutrino identity.

3. DETERMINATION OF THE SPACE-TIME STRUCTURE OF NEUTRAL CURRENTS

In contrast to Section 2, in this section we deal with results which are obtained from common fits of the ν and $\bar{\nu}$ data. This can be done in the frame of specific models, and allows severe tests on the validity of the models. Compared to fits of Section 2, the errors on the fit parameters are greatly reduced since the information on both the cross-section ratios and the y -distributions is combined, and the statistical weight of the total data sample is used.

For common fits the simple CC y -distribution with $\alpha_{CC} = \bar{\alpha}_{CC}$ as used in Eq. 1 is no longer adequate for the statistical accuracy of our total data sample. We have adopted a parametrization which takes for CC (but not for NC) both the deviation of iron from an isoscalar target and the effect of the strange sea into account:

$$\left. \begin{aligned} \frac{NC}{CC}(y) &= \frac{g_L + g_R(1-y)^2 \left[+g_{SP}y^2 \right]}{f_L + f_R(1-y)^2} && \text{for } \nu \\ &= \frac{g_L(1-y)^2 + g_R \left[+g_{SP}y^2 \right]}{\bar{f}_L(1-y)^2 + \bar{f}_R} && \text{for } \bar{\nu} \end{aligned} \right\} (2)$$

g_L and g_R denote the effective contributions from left- and right-handed NC for a target of iron nuclei. g_L and g_R are the same for ν and $\bar{\nu}$ NC interactions, whereas the equivalent parameters for CC are slightly different for ν and $\bar{\nu}$ interactions. Starting from

$$\frac{\int x(\bar{u} + \bar{d} + 2\bar{s})dx}{\int x(u + d)dx} = \alpha = 0.10 \text{ } ^3) \text{ and}$$

$$\frac{\int x2\bar{s} dx}{\int x(u + d)dx} = 0.03 \text{ } ^5)$$

we arrive in the frame of the quark-parton model as described for example by Sehgal⁶⁾ to the coefficients $f_L = 1.05$, $f_R = 0.07$, $\bar{f}_L = 0.98$ and $\bar{f}_R = 0.10$, which we have used as input parameters for the description of the y -distribution of CC interactions on iron nuclei.

3.1 S or P couplings in the NC structure

An S or P coupling in the NC structure shows up as a y^2 term in the y -distribution which is expected to be determined with good sensitivity. Adding in Eq. 2 both for ν and $\bar{\nu}$ a term $g_{SP}y^2$ in the NC y -distribution we find

$$\frac{g_{SP}}{g_L + g_R} = 0.02 \pm 0.07(0.05).$$

This result puts an upper limit of 16% on the intensity of scalar or pseudoscalar terms with respect to the V, A terms, at the 95% confidence level. Therefore, we restrict the further analysis to V, A couplings only ($g_{SP} = 0$).

3.2 The V, A structure of the NC interaction

In the quark-parton model, g_L is to be understood as the sum of the contributions of the V-A current from quarks, and the V+A current from antiquarks, with the reverse true for g_R . We find with Eq. 2

$$\left. \begin{aligned} g_L &= 0.300 \pm 0.012(0.005) \\ g_R &= 0.050 \pm 0.005(0.004) \end{aligned} \right\} \text{ with } \alpha = 0.10$$

In order to decide whether the NC interaction has pure V-A coupling, we compare the measured shape parameter of the NC y -distribution, $g_R/g_L = 0.167 \pm 0.018$, with the one we expect for pure V-A coupling: $\int x(\bar{u} + \bar{d} + \bar{s})dx / \int x(u + d) dx = 0.085$, with the assumptions stated above. This result rules out a pure V-A structure of the NC, and establishes a V+A admixture with a significance of more than four standard deviations. This significance is independent of the assumption on α within the range $0.05 < \alpha < 0.20$.

Fig. 4 provides a graphical illustration of the experimental result and its significance in discriminating between different hypotheses. It gives the contribution of the left- and right-handed NC coupling as predicted by V-A, pure V and A, and V+A. The experimental point rules out unambiguously V+A as well as pure V and pure A coupling. Pure V-A coupling is ruled out at the level of four standard deviations.

3.3 The Weinberg-Salam model

In this model one single parameter, $\sin^2\theta_w$, determines both the absolute NC cross-section and its y -distribution. We have fitted our data expressing g_L and g_R of Eq. 2 as functions of $\sin^2\theta_w$ as outlined for example by Sehgal⁶⁾. The deviation of iron from an isoscalar target and the effect of the strange sea have also been taken into account for the NC interaction. The result of the fit is shown in Fig. 3 as a solid line. Apparently, the data are well described by the Weinberg-Salam model both in the absolute cross-section and in the y -distribution, if $\sin^2\theta_w = 0.24 \pm 0.02(0.007)$. The quoted overall error is much larger than the statistical error, because it

includes in addition to the estimate of the systematic error, an uncertainty of the antiquark-quark ratio in the range $0.05 < \alpha < 0.20$. To show the agreement between the data and the Weinberg-Salam model we compare in Table 3 the measured values of R_ν , $R_{\bar{\nu}}$, α_{NC} and $\bar{\alpha}_{NC}$ determined from separate fits of the ν and $\bar{\nu}$ data, and of g_L and g_R determined from a common fit, with the predictions of the Weinberg-Salam model for $\sin^2\theta_w = 0.24 \pm 0.02$.

The Weinberg-Salam prediction is also included in Fig. 4, with $\alpha = 0.10$. The experimental point has a distance of about one standard deviation to the Weinberg-Salam line when taking the overall error. As a consistency check, we have performed a fit with $\sin^2\theta_w$ and α as free parameters. The fit reproduces the data best with $\alpha = 0.16 \pm 0.05$, and with $\sin^2\theta_w$ unchanged compared to the one-parameter fit.

Our results are in good agreement with recent results of the HWPF group⁷⁾, obtained in ν and $\bar{\nu}$ wide-band beams, and of the CITF group⁸⁾. The latter group has analyzed narrow-band beam data with characteristics similar to our data.

We would like to thank our many technical collaborators, and the members of the SPS staff for the operation of the accelerator.

REFERENCES

1. M. Holder et al., Measurement of the neutral to charged current cross-section ratio for neutrino and antineutrino interactions, submitted to Phys. Lett. B.
2. M. Holder et al., A detector for high-energy neutrino interactions, submitted to Nucl. Instr. Meth.
3. M. Holder et al., Phys. Rev. Lett. 39, 433 (1977).
4. L. Wolfenstein, Nucl. Phys. B91, 95 (1975).
5. M. Holder et al., Phys. Lett. 69B, 377 (1977).
6. L.M. Sehgal, Nucl. Phys. B65, 141 (1973).
7. P. Wanderer et al., Measurement of the neutral current interactions of high energy neutrinos and antineutrinos, submitted to Phys. Rev. D.
8. F.S. Merritt et al., Differential cross-sections for inclusive neutral current interactions at high energies, preprint CALT 68-600.
F.S. Merritt et al., Determination of the V, A structure of the neutral current coupling, preprint CALT 68-601.

Table 1

Fit results for the NC to CC total cross-section ratios, without a cut-off in the hadron-energy. The errors include the estimate of the systematic error. For comparison, the statistical error is given in brackets.

	Neutrinos	Antineutrinos
$E < 100 \text{ GeV}$	$R_{\nu} = 0.296 \pm 0.013(0.010)$ $\langle E_{\nu} \rangle = 60 \text{ GeV}$	$R_{\bar{\nu}} = 0.34 \pm 0.03(0.019)$ $\langle E_{\bar{\nu}} \rangle = 60 \text{ GeV}$
$E > 100 \text{ GeV}$	$R_{\nu} = 0.293 \pm 0.017(0.012)$ $\langle E_{\nu} \rangle = 150 \text{ GeV}$	$R_{\bar{\nu}} = 0.35 \pm 0.06(0.043)$ $\langle E_{\bar{\nu}} \rangle = 150 \text{ GeV}$
$\frac{R(E > 100 \text{ GeV})}{R(E < 100 \text{ GeV})}$	$0.99 \pm 0.07(0.06)$	$1.03 \pm 0.18(0.14)$
all energies	$R_{\nu} = 0.295 \pm 0.010(0.006)$ $\langle E_{\nu} \rangle = 110 \text{ GeV}$	$R_{\bar{\nu}} = 0.34 \pm 0.03(0.017)$ $\langle E_{\bar{\nu}} \rangle = 90 \text{ GeV}$

Table 2

Fit results for the shape parameter α_{NC} of the NC y -distribution. The errors include the estimate of the systematic error. For comparison, the statistical error is given in brackets.

	Neutrinos	Antineutrinos
$\alpha_{\text{CC}} = \bar{\alpha}_{\text{CC}} = 0.10$	$\alpha_{\text{NC}} = 0.19 \pm 0.18(0.16)$ $\alpha_{\text{NC}} - \alpha_{\text{CC}} = 0.09 \pm 0.18$	$\bar{\alpha}_{\text{NC}} = 0.20 \pm 0.07(0.06)$ $\bar{\alpha}_{\text{NC}} - \bar{\alpha}_{\text{CC}} = 0.10 \pm 0.07$
$\alpha_{\text{CC}} = \bar{\alpha}_{\text{CC}} = 0.15$	$\alpha_{\text{NC}} = 0.24 \pm 0.19(0.17)$ $\alpha_{\text{NC}} - \alpha_{\text{CC}} = 0.09 \pm 0.19$	$\bar{\alpha}_{\text{NC}} = 0.29 \pm 0.11(0.10)$ $\bar{\alpha}_{\text{NC}} - \bar{\alpha}_{\text{CC}} = 0.14 \pm 0.11$

TABLE 3

Comparison between the results of this experiment and the predictions of the Weinberg-Salam model.

		Experiment	Weinberg-Salam model with $\sin^2\theta_w = 0.24 \pm 0.02$
Separate fits of ν and $\bar{\nu}$ data, with $\alpha_{CC} = \bar{\alpha}_{CC} = 0.10$	$R_{\nu} \left. \vphantom{R_{\nu}} \right\} E_H > 0$	0.295 ± 0.010	0.295 ± 0.013
	$R_{\bar{\nu}} \left. \vphantom{R_{\bar{\nu}}} \right\} E_H > 0$	0.34 ± 0.03	0.390 ± 0.003
	α_{NC}	0.19 ± 0.18	0.19 ± 0.03
	$\bar{\alpha}_{NC}$	0.20 ± 0.07	0.19 ± 0.03
Common fit, with $\alpha = 0.10$	g_L	0.300 ± 0.012	0.301 ± 0.015
	g_R	0.050 ± 0.005	0.057 ± 0.004

FIGURE CAPTIONS

- Fig. 1 : Monte Carlo simulation of the reconstructed neutrino energy for neutral current events. The fiducial region (radial distance less than 1.6 m) is subdivided into four radial bins of 40 cm each. The plotted data shows neutrino events.
- Fig. 2 : Hadron-energy distributions of corrected NC and CC events, for all four bins of the radial distance, for neutrinos (Fig. 2a) and antineutrinos (Fig. 2b).
- Fig. 3 : Ratio of the NC to CC cross-sections as a function of the hadron-energy, for all four bins of the radial distance, for neutrinos (Fig. 3a) and antineutrinos (Fig. 3b). The solid line denotes the best fit of the Weinberg-Salam model, with $\sin^2\theta_W = 0.24$. For comparison, the Weinberg-Salam prediction is also given for $\sin^2\theta_W = 0.35$ (dashed line). The dotted line represents the prediction of pure V-A coupling.
- Fig. 3 : Graphical illustration of the left-handed versus right-handed NC coupling parameters g_L and g_R . The relative antiquark-quark ratio is assumed to be $\alpha = 0.10$. The deviation of iron from an isoscalar target and the effect of the strange sea are taken into account. The experimental point is shown together with the three standard deviation contour (statistical error). In addition the predictions of V-A, pure V and A, V+A, and the Weinberg-Salam model are given.

MONTE CARLO NEUTRINO EVENTS

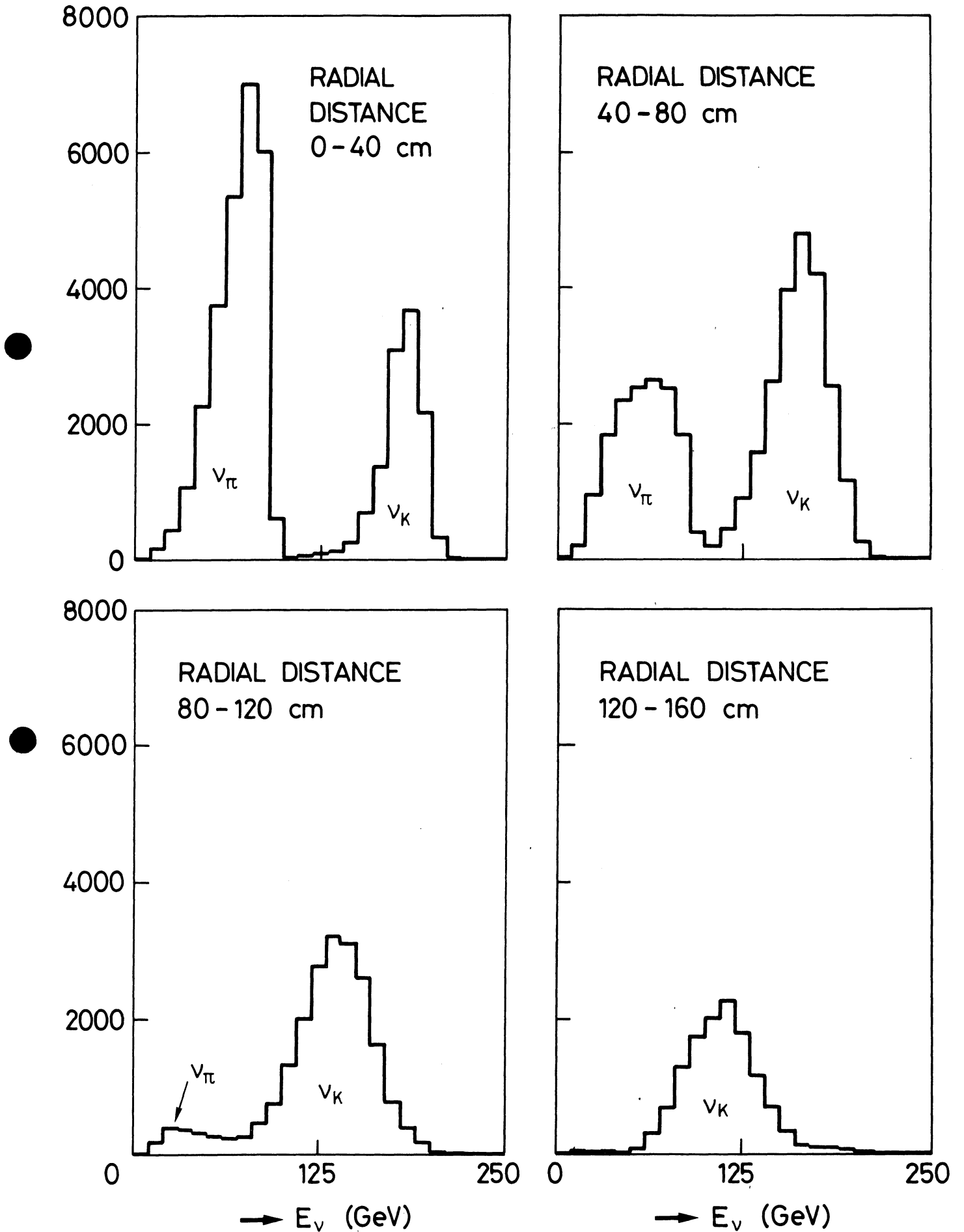


Fig. 1

NEUTRINO EVENTS

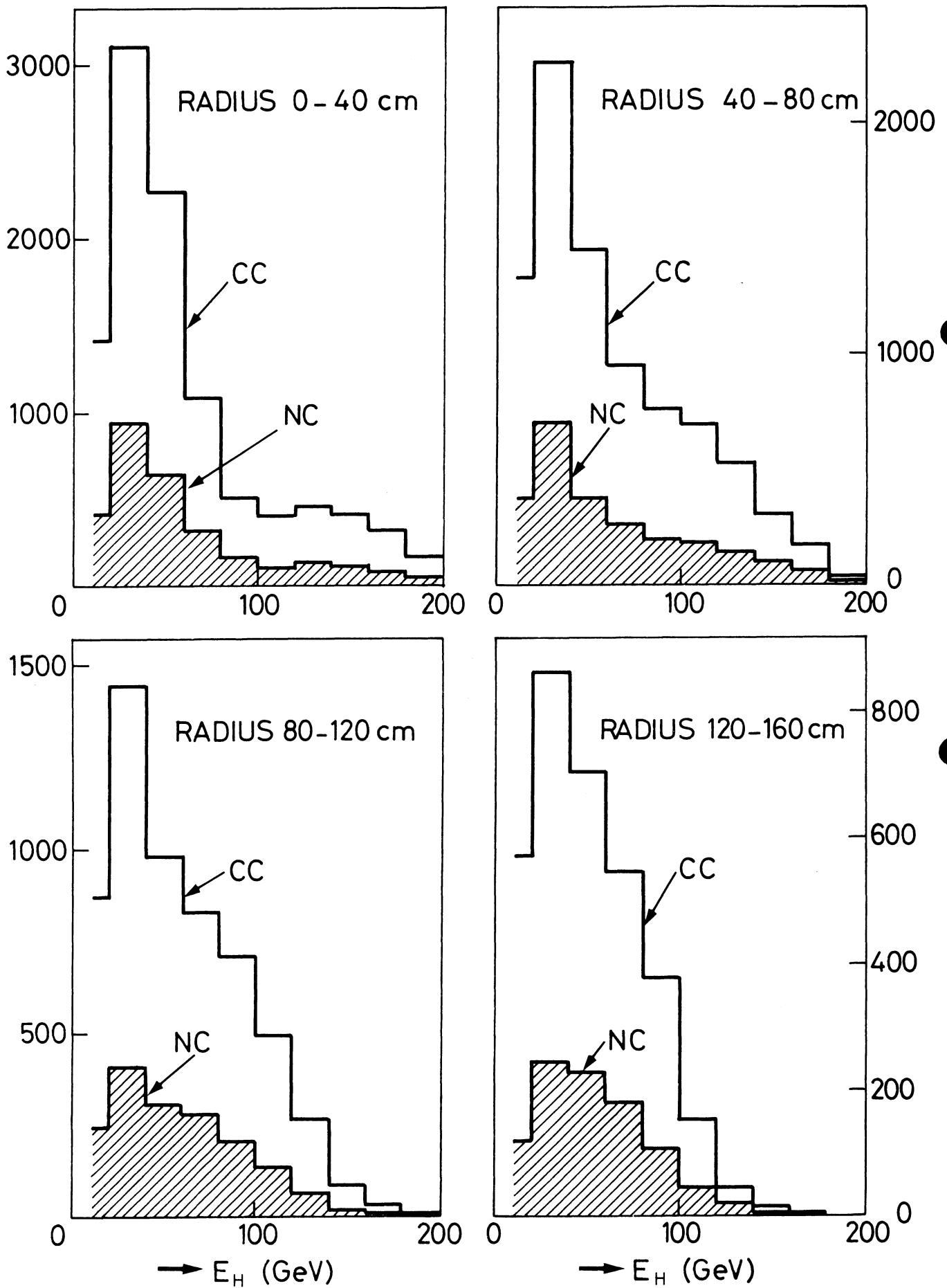


Fig. 2a

ANTINEUTRINO EVENTS

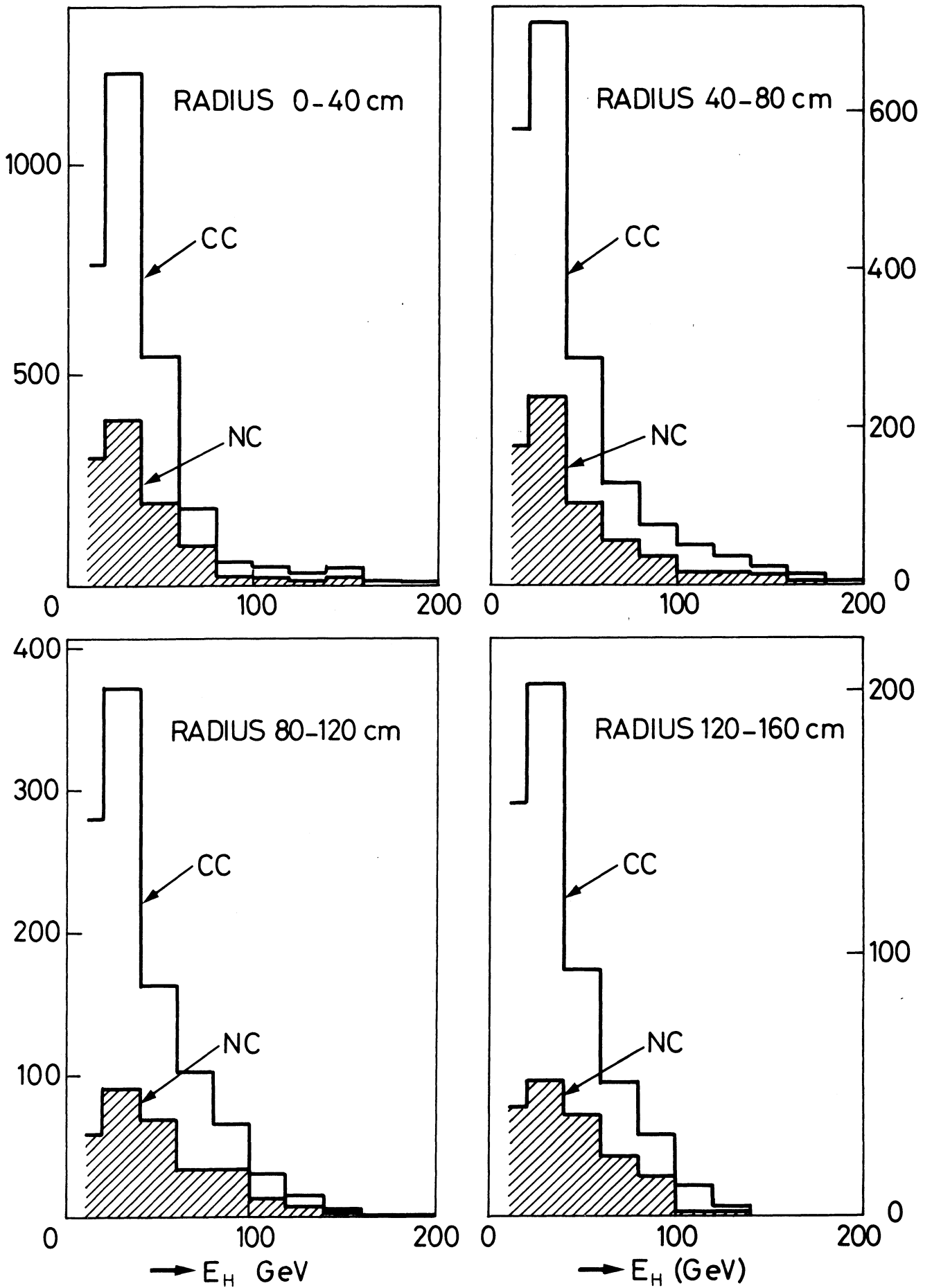


Fig. 2b

$\frac{NC}{CC}$ FOR NEUTRINOS

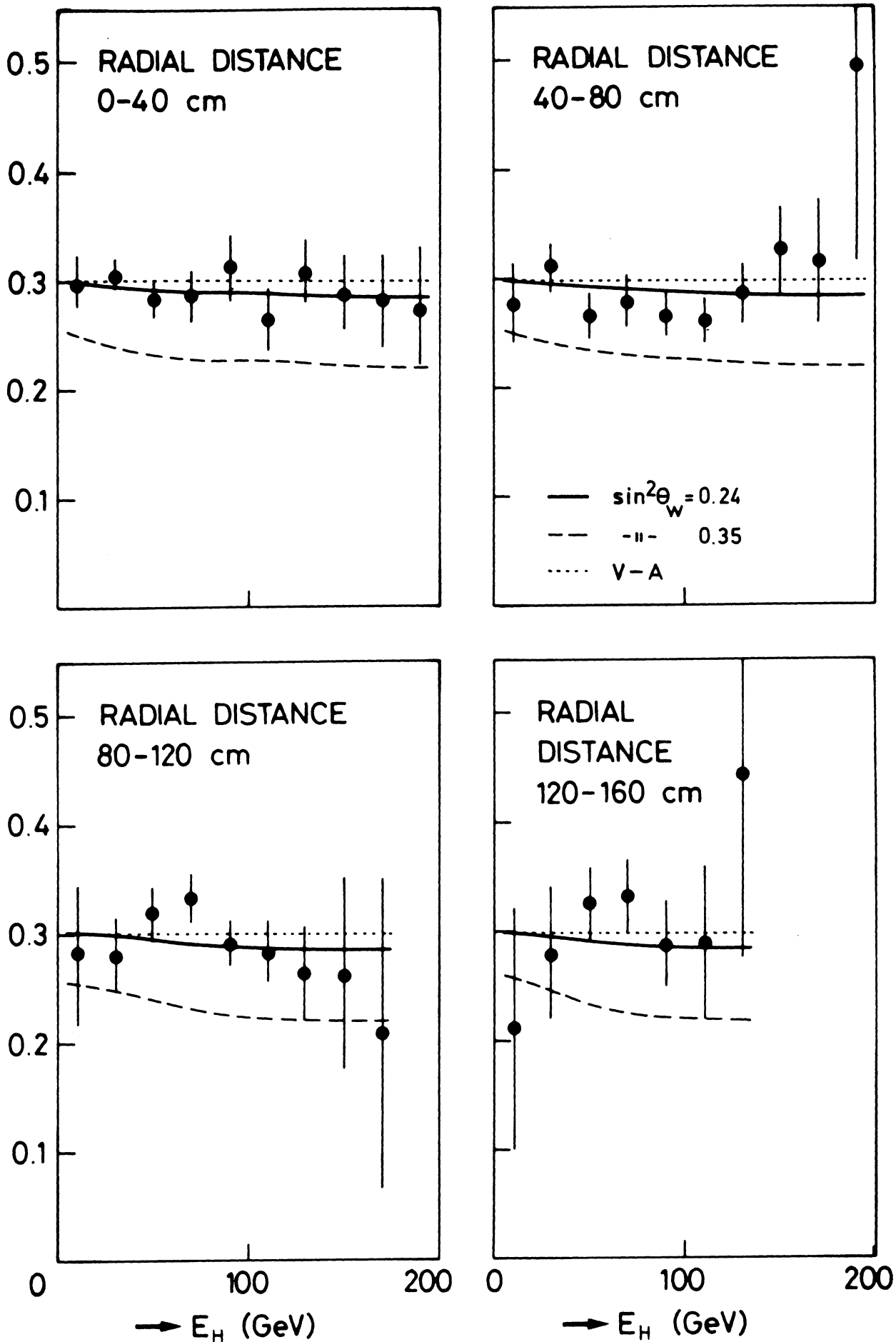


Fig. 3a

$\frac{NC}{CC}$ FOR ANTINEUTRINOS

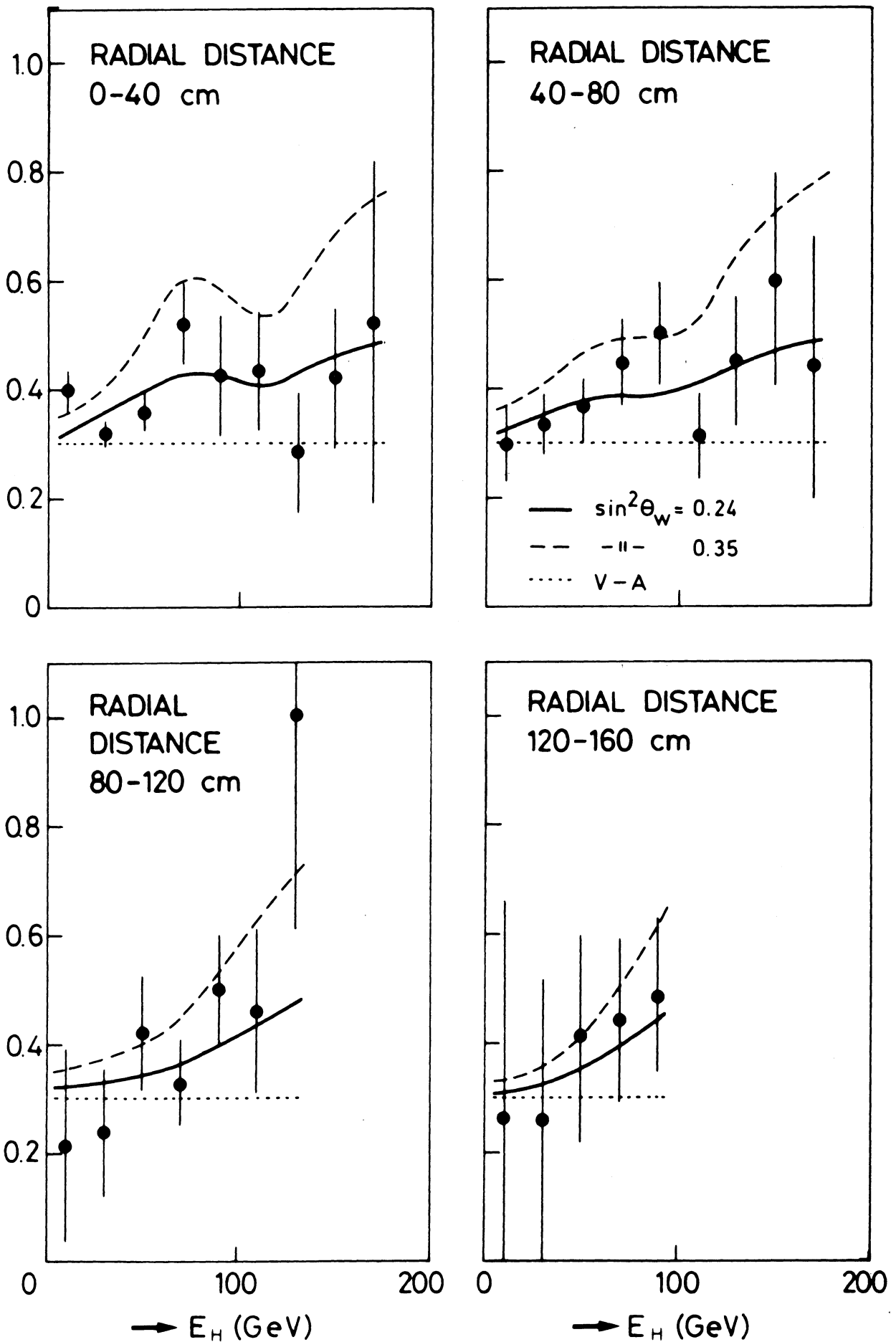


Fig. 3b

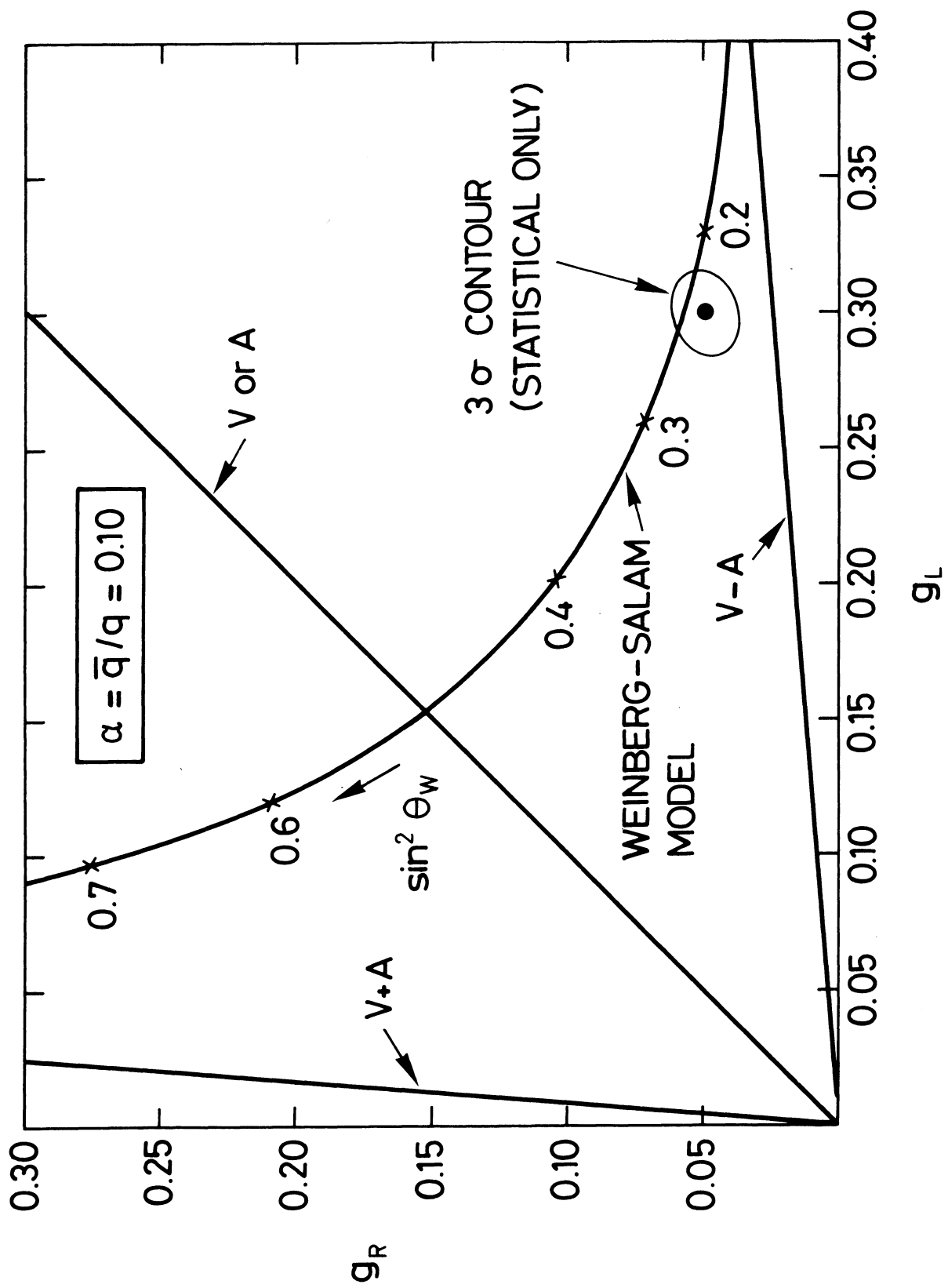


Fig. 4